High-efficiency 5000 lines/mm multilayer-coated blazed grating for EUV wavelengths

Dmitriy L. Voronov,[1,*] Minseung Ahn,[2] Erik H. Anderson,[1] Rossana Cambie,[1] Chih-Hao Chang,[2] Eric M. Gullikson,[1] Ralf K. Heilmann,[2] Farhad Salmassi,[1] Mark L. Schattenburg,[2] Tony Warwick,[1] Valeriy V. Yashchuk,[1] Lucas Zipp,[1] and Howard A. Padmore[1]

[1]*Lawrence Berkeley National Laboratory, 1 Cyclotron Road, Berkeley, CA 94720*

[2]*Space Nanotechnology Laboratory, Massachusetts Institute of Technology, 70 Vassar St., Cambridge, MA 02139*

[*]*Corresponding author: dlvoronov@lbl.gov*

Volume x-ray gratings consisting of a multilayer coating deposited on a blazed substrate can diffract with very high efficiency even in high orders if diffraction conditions in-plane (grating) and out-of-plane (Bragg multilayer) are met simultaneously. This remarkable property however depends critically on the ability to create a structure with near atomic perfection. In this work we report on a method to produce these structures. We report measurements that show, for a 5000 l/mm grating diffracting in the 3rd order, a diffraction efficiency of 37.6% at a wavelength of 13.6 nm, close to the theoretical maximum. This work now shows a direct route to achieving high diffraction efficiency in high order at wavelengths throughout the soft x-ray energy range.

OSIS codes: 050.1950, 120.6660, 340.7480, 230.4170, 310.1860

Multilayer (ML) coated blazed gratings seem to be the best choice [1] for many high-resolution soft x-ray spectroscopy techniques such as Resonance Inelastic X-Ray Scattering (RIXS) [2], which require high spectral resolution (10^4-10^6) combined with high efficiency. Such gratings should have a high groove density and operate in a high diffraction order because resolution depends directly on the *m/d* ratio (for a fixed grating size), where *m* is a blazed order, and *d* is the grating period. Moreover, high dispersion of the gratings with a large effective groove density allows the use of larger size slits, providing more light through a spectrograph or monochromator. A multilayer coating provides high grating efficiency and moves the spectrometer design away from grazing incidence. This reduces problems of geometric aberration and increases the grating acceptance, thus increasing throughput while decreasing the dimensions of the whole system [3].

In order to realize the advantages of ML blazed gratings in the EUV and soft x-ray range, saw-tooth substrates of very high quality are required. The smoothness of the facet surface and the profile of the grooves are the main concerns [4]. The best EUV blazed gratings have been fabricated with interference lithography combined with ion-beam etching [5, 6], or gray-scale e-beam lithography [7]. Efficiency of 41% has been obtained in 1st order diffraction at the wavelength of 12.5 nm with a 1000 groove/mm grating [7]. A denser 2400 grooves/mm grating has demonstrated efficiency in the second diffraction order of 36.2% at a wavelength of 15.79 nm [5], and 29.9% was achieved for a second-order grating with the groove density of 3000 grooves/mm [6]. These spectacular achievements show that the measured efficiency of the gratings is nevertheless significantly below the theoretical prediction, and technological challenges increase significantly for high groove density and high orders.

We believe that wet anisotropic etch of silicon is the most promising technique for high-resolution grating fabrication [8]. The process can provide both a triangular groove profile and an

atomically smooth surface of the blazed facets, due to crystal lattice perfection and the high anisotropy of the etch. This technique has been successfully applied to fabricate hard x-ray blazed gratings operating at grazing incidence [9]. A first attempt to fabricate a ML coated blazed grating for the soft x-rays showed that thorough optimization of the etch process is necessary to realize the advantages of the anisotropic etch approach [10]. Here we describe the fabrication process of a EUV blazed grating with effective groove density, *m/d*, of 15,000 lines/mm, and present measurements of efficiency of the grating coated with a Mo/Si multilayer.

The saw-tooth gratings were fabricated by KOH etching of asymmetrically cut silicon single crystals. Float zone (111) silicon wafers with a 6-degree mis-cut towards the [112] direction were used. After low-stress CVD silicon nitride deposition, anti-reflection coating (ARC) and photoresist spinning the wafers were patterned with scanning beam interference lithography [11]. Then the 200 nm period pattern was transferred to the nitride layer with an O_2 and CF_4 reactive ion etch. The wet etch of the samples was performed in 20% KOH solution stirred intensively at room temperature.

The SEM image of the gratings after the etching and nitride mask strip is shown in Fig.1a. The grating grooves consist of 6-degree tilted blazed facets with silicon nubs which are also shaped with {111} sidewalls. The surface of the blazed facets consists of atomically smooth (111) terraces and atomic steps (Fig. 2a). This kind of morphology is inherent for anisotropic etch because of the step-flow mechanism of the etch process [12]. Net roughness of the surface is defined by step density which in its turn depends on anisotropy of the reaction. AFM measurements showed roughness below 0.3 nm rms measured over a $1\times1\ \mu m^2$ area. This is close to the silicon lattice spacing in the (111) direction and indeed many of the AFM images showed clear evidence of (111) terraces and steps.

The silicon nubs remaining after the etch step must be removed before multilayer deposition, otherwise they can cause significant perturbation of the multilayer structure [13]. We used chemical oxidation of silicon with Piranha (H_2SO_4+H_2O_2) followed by oxide etch with HF as a nub removal process. Each oxidation/oxide etch cycle removes approximately 0.5 nm thick silicon layer. In total 26 cycles were applied in order to remove the 25 nm wide nubs and to get the groove profile close to a triangle (Fig. 3). Since cleanliness of the silicon surface is crucial, we performed an additional RCA clean of the samples before the Piranha/HF cycles as well as multiple de-ionized water rinses of the samples after each acid bath. The nub removal process results in a slight increase of high spatial frequency component of surface roughness (Fig. 2b) which is easily smoothed out by the multilayer deposition step that follows (Fig. 2c).

The multilayer, composed of 30 Mo/Si bilayers, was deposited onto the blazed grating substrates by dc-magnetron sputtering. The multilayer period was targeted to 7.2 nm in order to bring the 3rd diffraction order of the grating to the blaze condition and at the same time satisfy the first order Bragg condition for the multilayer. The groove profile of the grating changes significantly during the course of the deposition. Fig. 1c shows a cross-section TEM image of the multilayer coated grating, and Fig. 3 shows the AFM measurements of the average groove profile before and after deposition of the multilayer. Coating causes the surface of the blazed facets to become slightly convex and the apexes of the triangle groove to become rounded significantly.

The diffraction efficiency of the multilayer coated blazed grating was measured at the Advanced Light Source beamline 6.3.2 two-axis diffractometer [14]. The incident angle was set to 11° from the grating surface normal and an angular resolution of 0.12 degrees was used for the detector axis. The detector scans over the diffraction angle were performed at the wavelengths

between 12.7 nm and 15.0 nm with an increment of 0.1 nm. The data were normalized to the direct beam measured over the wavelength range.

Fig. 4 shows the diffraction from the Mo/Si-30 coated grating at the wavelength of 13.6 nm. The blazed 3rd diffraction order demonstrates efficiency as high as 37.6%, and the non-blazed orders are well suppressed. Fig. 5 shows experimental and simulated efficiency of the 3rd order versus the wavelength. Simulations were performed with a commercial code that solves Maxwell's equations for a period boundary [15]; this code was extensively benchmarked to other codes for the case of a perfect blazed structure [16-18] and found to agree to high precision, but it provided the additional flexibility to use measured shape information critical for modeling the effect of imperfections. These simulations reveal that the experimental substrate groove profile (dashed curve) provides a lower grating efficiency than the ideal one. In addition, smoothing of the groove profile by the multilayer has a negative impact on grating efficiency. The grating efficiency could be higher if the grating profile was preserved during the multilayer deposition. The rounding is caused by both the geometry of the magnetron sputtering used for multilayer deposition as well as re-sputtering processes and surface atom mobility which results in smoothing high spatial frequency features of the surface topography. One can expect that use of multilayer deposition with a collimated atomic flux would reduce rounding significantly and improve the grating efficiency.

In summary, we developed a process for fabrication of high quality EUV diffraction gratings with an effective groove density of 15,000 lines/mm. Substrate blazed gratings were made by scanning beam interference lithography and anisotropic KOH etching of silicon. The optimized anisotropic etching provides excellent control of the slope of blazed facets, high smoothness of the facet surface, and very short anti-blazed facets. A new nub removal step provides a triangular substrate groove profile which is close to the ideal one. The grating coated with Mo/Si-30 multilayer

demonstrated an efficiency of 37.6% in the 3rd diffraction order at 13.6 nm wavelength. The triangular substrate groove profile suffers some smoothing during the ML deposition with dc-magnetron sputtering. It may be that collimated deposition of the multilayer could address this issue. The combination of our method for producing near atomically perfect blazed substrates with collimated sputter coating opens up the prospect of highly efficient high order diffraction gratings for the whole of the soft x-ray energy region. Applications include ultra-high resolution spectroscopy as well as pulse compression of chirped x-ray beams.

This work was supported by the US Department of Energy under contract number DE-AC02-05CH11231.

References

1. D. L. Voronov, R. Cambie, R. M. Feshchenko, E. Gullikson, H. A. Padmore, A. V. Vinogradov, V. V. Yashchuk, "Development of an ultra-high resolution diffraction grating for soft x-rays," Proc. SPIE **6705**, 67050E-1 - 67050E-12 (2007).
2. *Proceedings of Workshop on Soft X-Ray Science in the Next Millennium: The Future of Photon-In/Photon-Out Experiments (Pikeville, Tennessee, 2000),* http://www.phys.utk.edu/WPWebSite/ewp_workshop_XRay_Report.pdf
3. T. Warwick, H. A. Padmore, D. Voronov, and V. Yashchuk, "A soft x-ray spectrometer using a highly dispersive multilayer grating," presented at the Tenth International Conference on Synchrotron Radiation Instrumentation, Melbourne, Victoria, Australia, 27 September – 2 October 2009.
4. J. C. Rife, T. W. Barbee Jr., W. R. Hunter, and R. G. Cruddace, "Performance of a Tungsten/Carbon Multilayer-Coated, Blazed Grating from 150 to 1700eV," Physica Scripta **41**, 418-421 (1990).
5. M. P. Kowalski, R. G. Cruddace, K. F. Heidemann, R. Lenke, H. Kierey, T. W. Barbee Jr., and W. R. Hunter, "Record high extreme-ultraviolet efficiency at near-normal incidence from a multilayer-coated polymer-overcoated blazed ion-etched holographic grating," Opt. Lett. **29**(24), 2914-2916 (2004).
6. H. Lin, L. Zhang, L. Li, Ch. Jin, H. Zhou, and T. Huo, "High-efficiency multilayer-coated ion-beam-etched blazed grating in the extreme-ultraviolet wavelength region", Opt. Lett. **33**(5), 485-487 (2008).

7. P. P. Naulleau, J. A. Liddle, E. H. Anderson, E. M. Gullikson, P. Mirkarimi, F. Salmassi, and E. Spiller, "Fabrication of high-efficiency multilayer-coated gratings for the EUV regime using e-beam patterned substrates," Opt. Comm. **229**, 109–116 (2004).
8. P. Philippe, S. Valette, O. Mata Mendez, and D. Maystre, "Wavelength demultiplexer: using echelette gratings on silicon substrate, " Appl. Opt. **24**(7), 1006-1011 (1985).
9. A. E. Franke, M. L. Schattenburg, E. M. Gullikson, J. Cottam, S. M. Kahn, and A., Rasmussen. "Super-smooth x-ray reflection grating fabrication," J. Vac. Sci. Technol. B **15**(6), 2940-2945 (1997).
10. J. H. Underwood, C. Kh. Malek, E. M. Gullikson, and M. Krumrey, "Mdtilayer-coated echelle gratings for soft x rays and extreme ultraviolet," Rev. Sci. Instrum. **66**(2), 2147-2150 (1995).
11. R. K. Heilmann, C. G. Chen, P. T. Konkola, and M. L. Schattenburg, "Dimensional metrology for nanometer-scale science and engineering: towards sub-nanometer accurate encoders," Nanotechnology **15**(10), S504-S511 (2004).
12. R. A. Wind, and M. A. Hines, "Macroscopic etch anisotropies and microscopic reaction mechanisms: a micromachined structure for the rapid assay of etchant anisotropy," Surf. Science **460**, 21–38 (2000).
13. D. L. Voronov, R. Cambie, E. M. Gullikson, V. V. Yashchuk, H. A. Padmore, Yu. P. Pershin, A. G. Ponomarenko, and V. V. Kondratenko, "Fabrication and characterization of a new high density Sc/Si multilayer sliced grating," Proc. SPIE **7077**, 707708-1 - 707708-12 (2008).
14. http://www-cxro.lbl.gov/beamlines/6.3.2
15. http://www.pcgrate.com
16. http://www.gsolver.com

17. M. Neviere , A.J.F. den Boggende , H.A. Padmore , K. Holfls, "Grating efficiency theory versus experimental data in extreme situations," Proc. SPIE **1545**, 76-87 (1991).

18. M. Neviere and F. Montiel, "Electromagnetic theory of multilayer gratings and zone plates" Proc. SPIE, Vol. **2805**, 176-183 (1996).

Figure captions

Fig. 1. SEM images of the 200 nm grating after KOH etch and nitride mask removal (a) and after nub removal (b), and cross-section TEM image of the grating coated with the Mo/Si multilayer (c).

Fig. 2. (Color online) Morphology of the groove surface of the blazed gratings after KOH etching (a), nub removal (b), and multilayer deposition (c).

Fig. 3. (Color online) Ideal profile of a silicon blazed grating (dashed line) and averaged profiles measured with AFM for the grating before (dotted line) and after (solid line) multilayer deposition.

Fig. 4. (Color online) Diffraction from the Mo/Si-30 multilayer coated grating measured at the incidence angle of 11° and the wavelength of 13.6 nm.

Fig. 5. (Color online) Experimental (circles) and simulated dependence of efficiency of the 3rd order on wavelength. The simulation was performed for an ideal groove profile (dash curve), and experimental profiles before (dot curve) and after (solid curve) deposition of the Mo/Si-30 multilayer. The interface width of 0.9 nm rms was taken into account for all the simulations.

Figure 1

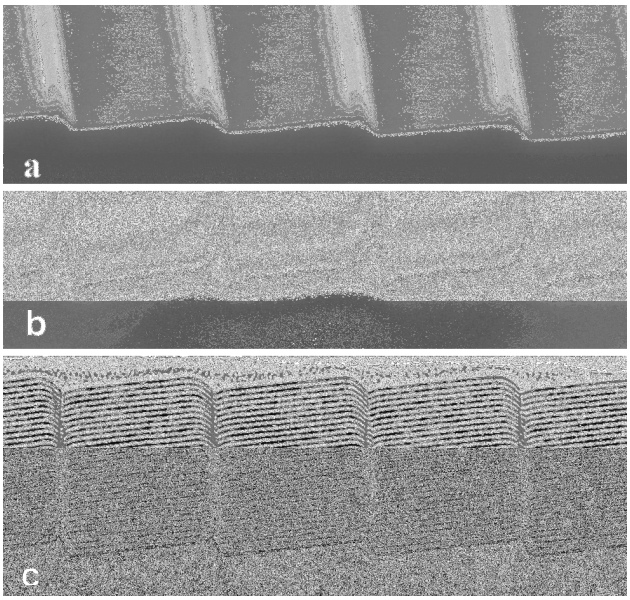

Figure 2

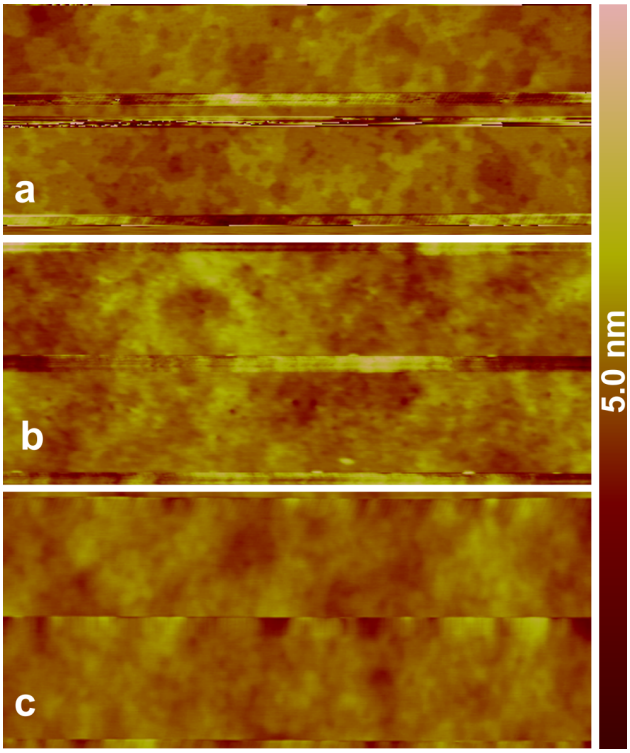

Figure 3

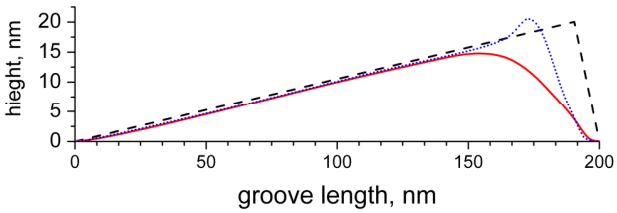

Figure 4

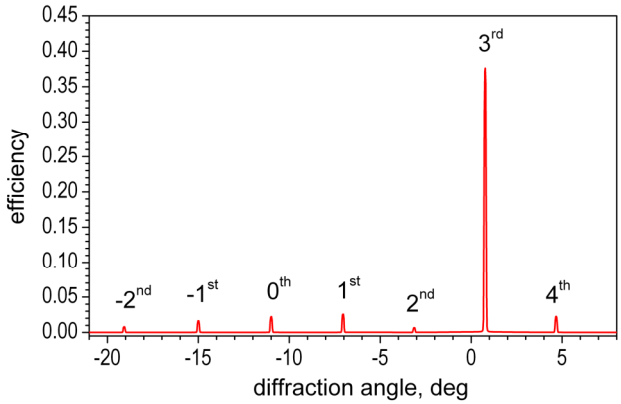
0.45
0.40
0.35
0.30
0.25
0.20
0.15
0.10
0.05
0.00
efficiency
-2nd
-1st
0th
1st
2nd
3rd
4th
-20
-15
-10
-5
0
5
diffraction angle, deg

Figure 5

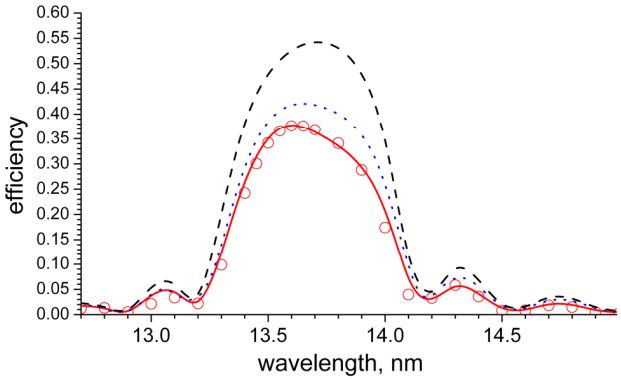
efficiency
0.60
0.55
0.50
0.45
0.40
0.35
0.30
0.25
0.20
0.15
0.10
0.05
0.00
13.0
13.5
14.0
14.5
wavelength, nm